

Low computational burden grid voltage estimation for grid connected voltage source converter-based power applications

Hosein Gholami-Khesht¹, Mohammad Monfared¹ ✉, Saeed Golestan²

¹Department of Electrical Engineering, Faculty of Engineering, Ferdowsi University of Mashhad, Mashhad, Iran

²Department of Electrical Engineering, Abadan Branch-Islamic Azad University, Abadan, Iran

✉ E-mail: m.monfared@um.ac.ir

ISSN 1755-4535

Received on 14th June 2014

Accepted on 11th November 2014

doi: 10.1049/iet-pel.2014.0466

www.ietdl.org

Abstract: This study presents a simple and efficient approach for grid voltage estimation based on the converter equations in the stationary reference frame. The proposed technique is adopted for the sensorless operation of the voltage source converter-based power conditioners. In this study, the effectiveness of the proposed estimation method when it is combined with a proportional-resonant (PR)-based current controller is investigated. When the PR controller is combined with the proposed voltage estimation technique, it offers an additional benefit, such that the grid voltage synchronisation is done without using any phase-locked loop or band-pass filter. The proposed sensorless control method shows an excellent steady-state and transient performance. It is proven through extensive simulations and experiments that the grid voltage estimation with a very low computational burden is achieved even when the grid voltage is distorted.

1 Introduction

Three-phase voltage source converters (VSCs) have become one of the main components of grid connected power applications such as renewable energy sources-based distributed power generation systems [1, 2], power quality and transmission equipment such as active power filter [3] and flexible ac transmission system controllers [4] because of various advantages they offer. The main advantages include the inherent converter current protection, fast dynamic response, accurate current regulation with low total harmonic distortion (THD), and controllable power factor. To extract maximum benefits from the VSCs, many strategies have been proposed to control them. Usually, three kinds of sensors for (i) grid voltage, (ii) grid current and (iii) DC-link voltage are required to implement a three-phase VSC controller. To reduce the cost and the size of grid connected converters and also improve the reliability, it is desirable to reduce the number of sensors. To accomplish this objective, the grid voltage sensor is usually replaced with a software algorithm which uses the converter parameters and other measured quantities as its inputs to estimate the instantaneous value of the AC voltage. So far many efforts have been done to present the grid voltage estimation algorithm, some of which are reviewed in the following.

The simplest voltage estimation method consists of adding the converter output voltage to the voltage drop on the AC filter. Despite its simplicity, it suffers from a serious drawback: it requires the differentiation operation on the grid current, and therefore is very sensitive to noise [5].

In voltage estimations based on instantaneous powers [5, 6], firstly, the instantaneous active and reactive powers are estimated using the measured currents, the measured DC-link voltage, the switching state, and the filter inductance. Afterwards, the grid voltages are calculated from the estimated powers and measured currents. Similar to the previous method, high frequency noises owing to the differentiation operation are amplified. Furthermore, the estimation accuracy is highly deteriorated, or even impossible, under light load conditions (near zero currents), because the estimated voltage is obtained from the division of the estimated power by the amplitude of the measured current.

One of the most common methods for grid voltage sensorless control and synchronisation is known as the virtual flux (VF) that

is based on the integral of the converter output voltage. This method does not require any differentiation or division in its structure. Besides, because of the intrinsic integration existed in the algorithm, the effect of distorted grid voltage on the control system is reduced [7–10]. Implementation of a perfect VF estimator is based on an ideal integrator and unfortunately is not practically possible. Noises and the DC offset in the measured currents cause drift and saturation. To overcome these problems, solutions such as low-pass filtering [7, 8], band-pass filtering [8, 9], and frequency-adaptive band-pass filtering [10] have been proposed. The steady-state error in estimated voltages, sensitivity to frequency variations, complicated structure, and necessity of a phase-locked loop (PLL) or a frequency-locked loop are considered as the main shortcomings of these methods.

Observer-based voltage estimation algorithms like Kalman filters [11], Luenberger observers [12], steepest descent techniques [13, 14] and other mathematical optimisations [15–19] have received much attention in recent years. These methods are used to estimate unknown parameters and states by minimising the error between the measured states and the predicted ones. Good dynamic and accuracy are some of their advantages, and complexity of estimation algorithms, difficulty of tuning the observer gain, and high computational burden are recognised as their serious disadvantages [11–19].

Voltage sensorless control methods based on the one-cycle control are proposed in [20–22], which have the benefits of simple structure and fast dynamic response because of continuous corrective action of analogue implementation. However, these techniques suffer from some serious drawbacks: (i) controller modification is not possible without hardware re-design because of analogue implementation; (ii) the assumption that the grid voltage amplitude is known and constant, (iii) the limited operation to the unity power factor and (iv) poor performance under light load conditions and when the converter operates in the inverting mode.

This paper proposes a simple and efficient method for grid voltage estimation that can be easily adopted in various control strategies of VSC applications. The proposed estimation method needs only a few simple operations such as sums and products, and does not require any integral, derivative or trigonometric operations in its structure.

This paper is organised as follows; in Sections 2 and 3, firstly, the converter system model is described. Afterwards, the proposed

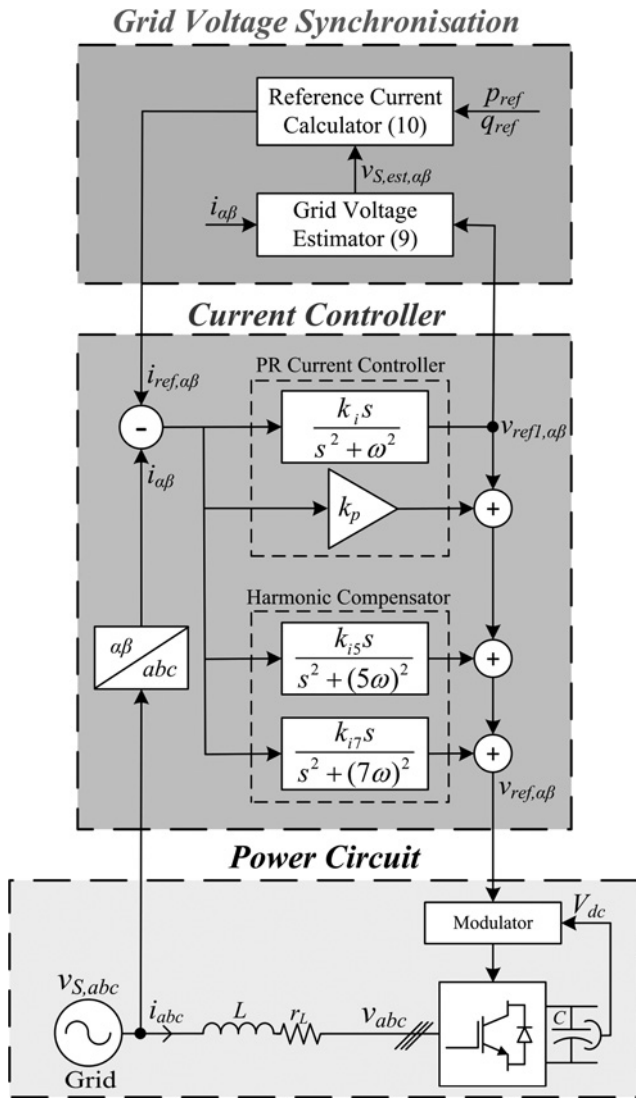


Fig. 1 Proposed control scheme for the grid connected VSC

voltage estimation method and the current regulation technique are presented. Moreover, Section 4 is prepared to verify the feasibility of the proposed method under various conditions through extensive simulation and experimental tests.

2 Proposed control scheme

The block diagram of the proposed voltage estimation and current control method is shown in Fig. 1, which consists of the current control loop and the sensorless grid voltage synchronisation, where the symbols are defined as follows:

- $v_{S,abc}$ i_{abc} three-phase grid voltages and currents
- v_{abc} three-phase converter AC-side output voltages
- $v_{S,\alpha\beta}$ $i_{\alpha\beta}$ two-phase grid voltages and currents under α - β frame
- $v_{\alpha\beta}$ two-phase converter AC-side output voltages under α - β frame
- $v_{S,est,\alpha\beta}$ two-phase estimated grid voltages under α - β frame
- $i_{ref,\alpha\beta}$ two-phase current references under α - β frame

- $v_{ref,\alpha\beta}$ two-phase voltage references under α - β frame
- $v_{ref1,\alpha\beta}$ two-phase outputs of the resonant part of the proportional-resonant (PR) controller under α - β frame
- p_{ref} q_{ref} active and reactive power references
- V_{dc} DC-link voltage
- L , r_L filter inductance and equivalent series resistance

The current control loop uses the PR controllers and harmonic compensators (HCs) to regulate the grid current and eliminate the low-order harmonic components [1, 23–33].

The PR-based current control is implemented in the stationary reference frame and provides a very high gain at its resonant frequency (grid fundamental frequency). Therefore, in this method, tracking of sinusoidal signals with zero steady-state error is achieved simply. Moreover, in this method, harmonic compensation is easily achieved with paralleling the PR controller with the HC network that includes resonators at the desired harmonic frequencies to be attenuated (here fifth and seventh). The HC network does not affect the performance of the PR controller and only have impact on frequencies close to its resonant frequency, also it can act on both positive and negative harmonic components without any change in its structure, which causes the PR controller with the HC network become a successful solution for high performance applications in networks with low-order harmonics.

2.1 Proposed voltage estimation method

In the stationary reference frame, the power-circuit dynamics of the grid connected VSC can be represented by the following model

$$v_{S\alpha\beta} = r_L i_{\alpha\beta} + L \frac{d}{dt} (i_{\alpha\beta}) + v_{\alpha\beta} \quad (1)$$

Grid voltage sensors can be easily replaced by a software algorithm that computes (1). Despite its simplicity, it requires the differentiation operation on the grid current which is very sensitive to noises, because the grid current includes low and high order harmonics because of switching operation and non-linear effects of the power converter system as written in the following equation

$$\begin{cases} i_a = \sum_{n=1,3,5,\dots} I_n \sin(n\omega t - \theta_n) \\ i_b = \sum_{n=1,3,5,\dots} I_n \sin(n\omega t - \theta_n - 2n\pi/3) \\ i_c = \sum_{n=1,3,5,\dots} I_n \sin(n\omega t - \theta_n + 2n\pi/3) \end{cases} \quad (2)$$

By applying the ‘Clarke’ transformation to above currents, the following orthogonal two-phase currents can be obtained (see (3)). The differentiation operation on the grid currents yields (see equation (4) at the bottom of the page)

To avoid problems of the differentiation operation on the grid currents (e.g. amplification of high frequency noises, difficulties of filtering and practical implementation, necessity of a high sampling frequency and dependency on the switching state, because high errors of the estimated values occur at the moment of switching), in this paper, it is proposed to replace the differentiation terms with the simple algebraic equations follows

$$\begin{cases} \frac{di_\alpha}{dt} \cong -\omega i_\beta \\ \frac{di_\beta}{dt} \cong \omega i_\alpha \end{cases} \quad (5)$$

Regarding (3) and (4), the above substitution is true for the

$$\begin{cases} i_\alpha = \overbrace{I_1 \sin(\omega t - \theta_1)}^{\text{fundamental component}} + \overbrace{\sum_{n=5,7,11,\dots} I_n \sin(n\omega t - \theta_n)}^{\text{harmonic components}} \\ i_\beta = \overbrace{-I_1 \cos(\omega t - \theta_1)}^{\text{fundamental component}} - \overbrace{\sum_{n=7,13,\dots} I_n \cos(n\omega t - \theta_n) + \sum_{n=5,11,17,\dots} I_n \cos(n\omega t - \theta_n)}^{\text{harmonic components}} \end{cases} \quad (3)$$

fundamental component of the grid current as rewritten in the following equation

$$\begin{cases} \frac{di_{\alpha 1}}{dt} = -\omega i_{\beta 1} = \omega I_1 \cos(\omega t - \theta_1) \\ \frac{di_{\beta 1}}{dt} = \omega i_{\alpha 1} = \omega I_1 \sin(\omega t - \theta_1) \end{cases} \quad (6)$$

while higher-order components are attenuated by the factor $1/n$, as rewritten in (7) and (8). This offers some kind of switching harmonic filtering, which is desirable for practical implementation of the proposed voltage estimation method. It also greatly simplifies the filtering and extraction of the grid voltage fundamental component. (see (7) and (8))

In summary, by substituting (5) into the estimated voltage equation (1), the phase and amplitude of the fundamental component are preserved, while the amplitude of higher-order harmonics are attenuated, which is desirable for switching harmonic filtering. Consequently, the possibility of a perfect differentiation operation for practical implementation of the voltage estimator (1) is achieved, while simplicity of the voltage estimator is still held. Moreover, the voltage estimation is much less noisy thanks to the natural filtering behaviour of the proposed method.

Finally, the equations of the proposed voltage estimation method can be concluded as

$$\begin{cases} v_{S\alpha} = r_L i_{\alpha} - L\omega i_{\beta} + v_{\alpha} \\ v_{S\beta} = r_L i_{\beta} + L\omega i_{\alpha} + v_{\beta} \end{cases} \quad (9)$$

It is clear from (9) that the proposed voltage estimation is basically a simple algebraic equation that only includes a few operations, such as sums and products. Therefore, for the proposed voltage estimation, neither stability, nor convergence rate and conditions are defined. The estimation performance, in terms of accuracy, is only affected by the accuracy of the filter parameters. Therefore it is necessary to investigate the influence of the parameter mismatches on the performance of the voltage estimator. Due to the fact that the voltage drop on the filter impedance, in comparison to the converter output voltage, is small, the steady-state error for a wide range of parameter mismatches is negligible, as shown in Section 4.

2.2 Proposed grid voltage sensorless synchronisation method

As shown at the top of the block diagram of Fig. 1, the reference converter currents for the PR regulators are generated from the

estimated grid voltages and the reference powers, in accordance with the following

$$\begin{bmatrix} i_{ref,\alpha} \\ i_{ref,\beta} \end{bmatrix} = \frac{2}{3} \frac{1}{(v_{S,est,\alpha}^2 + v_{S,est,\beta}^2)} \begin{bmatrix} v_{S,est,\alpha} & v_{S,est,\beta} \\ v_{S,est,\beta} & -v_{S,est,\alpha} \end{bmatrix} \begin{bmatrix} P_{ref} \\ Q_{ref} \end{bmatrix} \quad (10)$$

In (10), $v_{S,est,\alpha}$ and $v_{S,est,\beta}$ are the estimated grid voltage components in the stationary ($\alpha\beta$) reference frame that are already calculated from (9).

Converter synchronisation and providing a sinusoidal template for the reference current generation is based on the fundamental grid voltage component. The synchronisation with the fundamental component is often done by using a PLL or a band-pass filter (BPF) which adds complexity and reduces the system dynamic response. In the proposed method, when the PR controller is combined with the proposed voltage estimation, grid voltage synchronisation is simply achieved without using any PLL or BPF as will be described.

As written in (9), the voltage estimator needs the converter output voltage as its input. In a pulse-width modulation (PWM)-VSC, it is possible to use the converter reference voltage instead of the actual converter voltage. This technique is simple and noise-resistant. Although, when the reference voltage is used, some error compensation schemes must also be used to obtain high accuracy, such as voltage limitation and PWM delay compensation. In the proposed voltage estimator, if the input signal to the modulator [sum of outputs of the PR controller and the HC-network (v_{ref})] is used as the input signal to the grid voltage estimator, then the actual grid voltage with all its harmonic contents will be estimated, which is not usually necessary. On the other hand, if only the output of the PR controller is used as the input signal to the estimator, the voltage estimator can successfully estimate the fundamental component of the distorted grid voltage, which is desirable for grid synchronisation purposes. This attractive feature is derived from the inherent nature of the PR controller and the HC, because of the output of the resonator at any desired harmonic frequency has information of the grid voltage at that harmonic frequency. Also, it is worth mentioning that, in the practical implementation and as shown in Fig. 1, $v_{ref,1}$ is chosen as the output of the resonator part of the PR controller and the effect of the proportional component is ignored. It is clear that at the steady-state condition, the proportional term is almost zero because of an insignificant error signal; therefore it has no contribution to the output of the PR controller. However, during transients, the proportional term may experience high amplitude and fast oscillations. Hence, it is obvious that a low-pass filter must be inserted before the grid voltage estimator to provide some kind of

$$\begin{cases} \frac{di_{\alpha}}{dt} = \overbrace{\omega I_1 \cos(\omega t - \theta_1)}^{\text{fundamental component}} + \overbrace{\sum_{n=5,7,11,\dots} n\omega I_n \cos(n\omega t - \theta_n)}^{\text{harmonic components}} \\ \frac{di_{\beta}}{dt} = \overbrace{\omega I_1 \sin(\omega t - \theta_1)}^{\text{fundamental component}} + \overbrace{\sum_{n=7,13,\dots} n\omega I_n \sin(n\omega t - \theta_n) - \sum_{n=5,11,17,\dots} n\omega I_n \sin(n\omega t - \theta_n)}^{\text{harmonic components}} \end{cases} \quad (4)$$

$$\begin{cases} \frac{1}{n} \left| \frac{di_{\alpha n}}{dt} \right| = \omega |i_{\beta n}| \\ \frac{di_{\alpha n}}{dt} = \sum_{n=5,7,11,\dots} n\omega I_n \cos(n\omega t - \theta_n) \\ \omega i_{\beta n} = -\sum_{n=7,13,\dots} I_n \omega \cos(n\omega t - \theta_n) + \sum_{n=5,11,17,\dots} I_n \omega \cos(n\omega t - \theta_n) \end{cases} \quad (7)$$

$$\begin{cases} \frac{1}{n} \left| \frac{di_{\beta n}}{dt} \right| = \omega |i_{\alpha n}| \\ \frac{di_{\beta n}}{dt} = \sum_{n=7,13,\dots} n\omega I_n \sin(n\omega t - \theta_n) - \sum_{n=5,11,17,\dots} n\omega I_n \sin(n\omega t - \theta_n) \\ \omega i_{\alpha n} = \sum_{n=5,7,11,\dots} I_n \omega \sin(n\omega t - \theta_n) \end{cases} \quad (8)$$

immunity to these oscillatory transients. Another wise solution is to exclude the effect of proportional term on the $v_{ref,1}$, fed to the estimator, at the expense of a bit longer time to bring back the estimated voltages to the real values in response to large transients. Indeed, by using this simple technique, resonant part of the PR controller has a dual role as controller and as a filter. Consequently, an additional filter to extract the fundamental component of grid voltage is not necessary anymore. In Section 4 and in Fig. 6a, successful operation of the voltage estimator to estimate the fundamental component of the distorted grid voltage is illustrated.

3 Controller parameters design

As already stated, the ideal resonators of PR controller and the HC network have an infinite gain only at their resonant frequency and do not affect the phase or gain at other frequencies. Indeed, practical implementation of the ideal PR controller or the HC network, owing to their infinite gain and high sensitivity to utility frequency variations is not possible [27–30]. Therefore, to overcome these problems, the non-ideal PR controller and the HC network are proposed as

$$\begin{cases} G_{PR}(s) = k_p + \frac{k_i \omega_c s}{s^2 + 2\omega_c s + \omega^2} \\ G_{HC}(s) = \sum_{h=5,7} \frac{k_{ih} \omega_c s}{s^2 + 2\omega_c s + (h\omega)^2} \end{cases} \quad (11)$$

where k_p , k_i , ω , ω_c and h are proportional gain, resonant gain, resonance frequency, cutoff frequency and harmonic order, respectively. Gains of the non-ideal PR and the HC are now finite but still relatively high to effectively eliminate the steady-state tracking errors. Another important feature of the non-ideal PR and HC is their wider bandwidth than ideal cases that can be useful for reducing the sensitivity to power grid frequency variations by appropriate selection of ω_c .

In the following, firstly, the design procedure of the PR controller and the HC in the frequency domain is presented. Afterwards, system stability margins are examined by means of the Bode-plot technique that confirms the effectiveness of the controller design process. Finally, in the last subsection, the effect of control delay in the system modelling and control design is investigated.

3.1 Design of PR controller

So far, many efforts have been done to design the PR controller and the HC network [27–33]. A simple and commonly used approach for this purpose is the conventional Bode-plot technique that represents the frequency response of the open-loop system [27–30, 32]. Neglecting the effect of HC network on the system dynamic, the block diagram of the current control loop in the Laplace domain is depicted in Fig. 2. Regarding to this figure, the loop gain is defined as

$$\begin{cases} G(s) = G_{PR}(s) \times G_P(s) \\ G_P(s) = \frac{1}{r_L + sL} \end{cases} \quad (12)$$

where $G_P(s)$ is the transfer function of the inductive filter. As

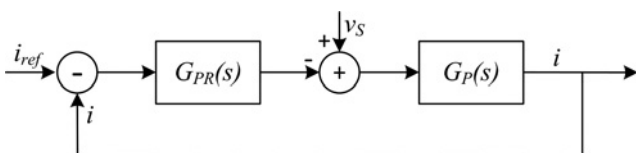


Fig. 2 Simplified block diagram of the current control loop

mentioned in earlier studies [23–33] and similar to the PI controller, k_p mainly determines the transient response of the controller, while k_i has effect on the steady-state error. Based on the analysis explained in these references, the controller parameters design can be summarised as following steps:

Step 1: Firstly, a small value for ω_c is selected. The lowest value is desirable to get low bandwidth for effective operation of HC and accurate grid synchronisation. However, the minimum possible value of ω_c is limited by the slower transient response and difficulty of implementation in some DSPs because of the coefficient quantisation and the round-off error [27–29], then a good compromise in our application is $\omega_c = 1$ rad/s.

Step 2: Afterwards, k_p is chosen such that the gain crossover frequency of $G(s)$, given by (12), becomes about one-tenth of the switching frequency to obtain both fast dynamic and switching noise immunity [30, 31]. Based on the mentioned analysis and this fact that the integral gain has almost no effect on the system dynamic, k_p can be obtained by solving the following equation

$$\begin{cases} |G(j\omega_g)| = 1 \\ k_i = 0 \\ \omega_g \cong 0.1\omega_{sw} \end{cases} \quad (13)$$

where ω_g and ω_{sw} are the decided gain crossover frequency of the loop gain and the switching frequency of the converter, respectively. A direct result of the above equation is as follows

$$k_p = \sqrt{r_L^2 + (L\omega_g)^2} \quad (14)$$

which with our parameters gives $k_p = 12$.

Step 3: Final step is to decide the proper value of k_i . Indeed, k_i must be selected sufficiently high to remove the steady-state errors at the cost of worse filtering and stability. Also, it is worth pointing out that the PR controller, unlike the PI, does not need any voltage feedforward for disturbance rejection; because, the high gain at resonant frequency provides an excellent disturbance rejection. Based on the mentioned analysis, k_i can be computed so that the following constraint is fulfilled

$$\angle G(j\omega_g) = PM - 180^\circ \quad (15)$$

where PM is a desired phase margin. Solving (15) with respect to k_i , yields

$$\begin{cases} k_i = \frac{k_p \tan(PM + \theta_p - 180^\circ) \left((\omega^2 - \omega_g^2)^2 + 4\omega_c^2 \omega_g^2 \right)}{\omega_c \omega_g (\omega^2 - \omega_g^2) - 2\omega_c^2 \omega_g^2 \tan(PM + \theta_p - 180^\circ)} \\ \theta_p = \arctan\left(\frac{L}{r_L}\right) \end{cases} \quad (16)$$

The resonant gain with the decided PM ($PM \cong 90^\circ$) is computed as $k_i = 5000$. This PM is higher than its desired value in most power electronic applications ($30^\circ < PM < 60^\circ$), because, as it will be shown, not considered aspects such as the control delay and the phase reduction because of the HC will reduce the PM.

3.2 Design of HC

In this paper and in order to immune the current controller from the grid voltage harmonic distortion, an HC including two modules tuned at the fifth and seventh harmonic frequencies are used. Because they are the most prominent harmonics in a practical three-phase power source spectrum as shown for our system in Fig. 6d. This consideration is an acceptable tradeoff between harmonic immunity, system complexity and control processing load [1, 25, 27–31]. In order to simplify the analysis and achieve

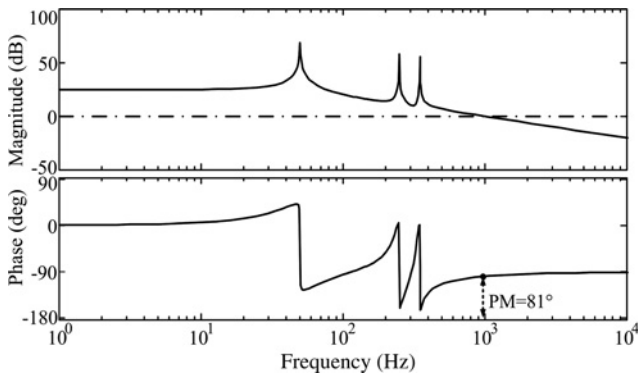


Fig. 3 Bode plot of loop gain $G(s)$ in presence of HC in parallel with PR

the same bandwidth for all resonators, several authors proposed that resonant gains for all resonators can be selected identical [29, 32]. Resonant gains must be selected as high as possible to ensure disturbance rejection and minimisation of steady-state errors with

regarding the system stability consideration. In this paper, resonator gains are selected as $k_{ih} = k_i = 5000$ for $h = 5$ and 7. Finally, in order to examine the system stability in presence of the HC, the Bode-plot of loop gain which includes the HC parallel with the PR controller is depicted in Fig. 3. As it can be seen, this design procedure results in a gain crossover frequency and PM of 976 Hz and 81° , respectively.

3.3 Effect of control delay

In digital implementation, there always exists a time delay (introduced by the analogue-to-digital converters, program execution and PWM) in the control loop. As analysed in [31], these delays cause extra loop phase lag that can affect the control performance and the system stability. Therefore it is necessary to check the system stability in the presence of delays in the system. A simple and efficient relation between the control delay and the system stability in terms of PM is presented by [31]

$$\Delta\text{PM} = -\omega_g T_d \quad (17)$$

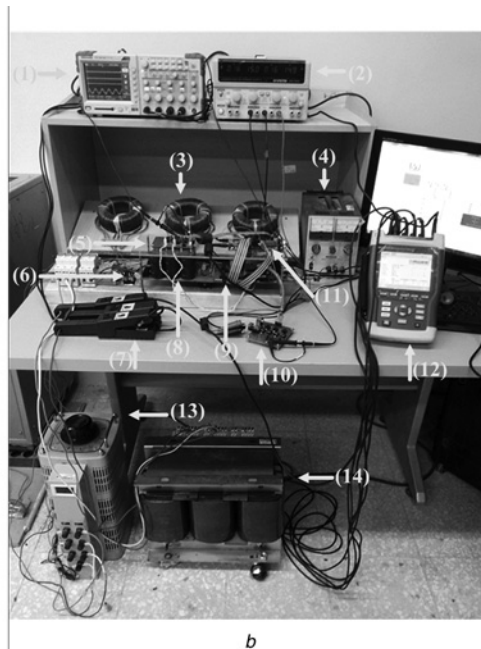
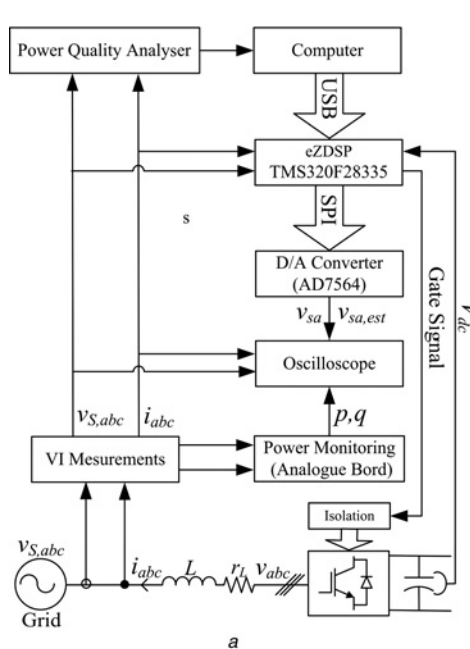


Fig. 4 Experimental test bench

a Schematic diagram of the experimental test bench

b Hardware setup: (1) oscilloscope (2) DC power supply (3) L-type filters (4) DC power supply (5) Digital to analogue (D/A) converter (AD7564) (6) three-phase diode bridge rectifier (7) current clamps (8) DC-link capacitors (9) VSC (10) power monitoring analogue board (AD633) (11) eZdsp TMS320F28335 (12) power quality analyser (13) three-phase auto-transformer and (14) three-phase transformer

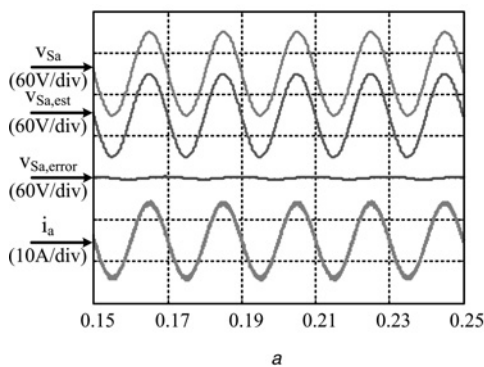


Fig. 5 Simulated steady-state performance of the proposed method

a Grid voltage and current

b Exchanged powers

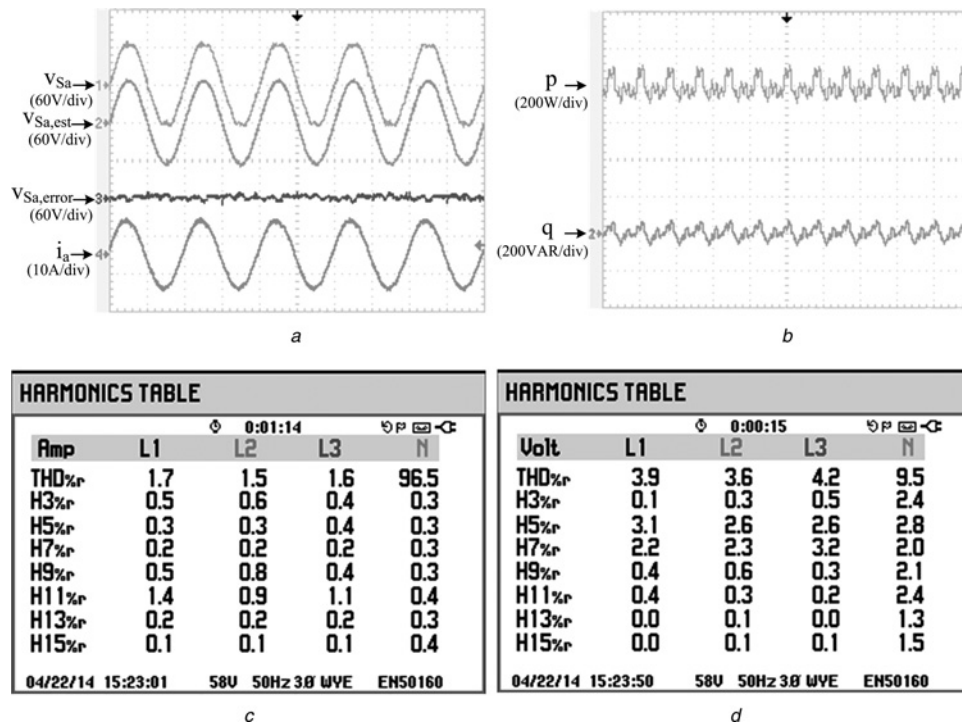


Fig. 6 Experimental steady-state performance of the proposed method under distorted grid voltages

- a Grid voltage and current
- b Exchanged powers
- c Harmonics table of grid current
- d Harmonics table of grid voltage

where ΔPM and T_d are reduction in the PM and the time delay. Here, $\omega_g = 976 \times 2\pi$ (rad/s), which means that, for one switching period delay, the new PM is 46° . The reduced PM is still adequate to ensure the system stability and avoid the oscillatory response. Different approaches for delay compensation and improving the reliability are suggested in [32, 33].

4 Performance validation

To verify the viability of the proposed sensorless control scheme, several simulation and experimental tests have been designed under various operating conditions. The simulation and experimental investigations have been conducted on a 1 kVA VSC. The main parameters of the simulated and experimental platform are as follows: grid voltage = 70 V(rms) at 50 Hz, filter nominal parameters $L = 2$ mH and $r_L = 0.7 \Omega$. The DC-link voltage is 140

V, and the carrier frequency for sinusoidal pulse width modulation (SPWM) generation is 10 kHz.

Simulation model has been established in Matlab/Simulink and the schematic diagram and an image of the experimental test bench are shown in Fig. 4. As depicted, the experimental setup includes a VSC, the TMS320F28335 digital signal controller (DSC) from Texas Instruments, a digital-to-analogue (D/A) converter (AD7564), the Fluke 435 power quality analyser, the power monitoring analogue board (composed of analogue multipliers AD633) to display the instantaneous powers. The DSC performs the proposed control scheme and sends waveforms of the estimated and measured grid voltages through the serial peripheral interface to the AD7564 serial D/A converter. The D/A converts these digital data to analogue signals to be displayed on the oscilloscope. It must be noted that in our experimental setup, a three-phase auto-transformer feeding a three-phase diode bridge rectifier have the role of DC power source as shown in Fig. 4b.

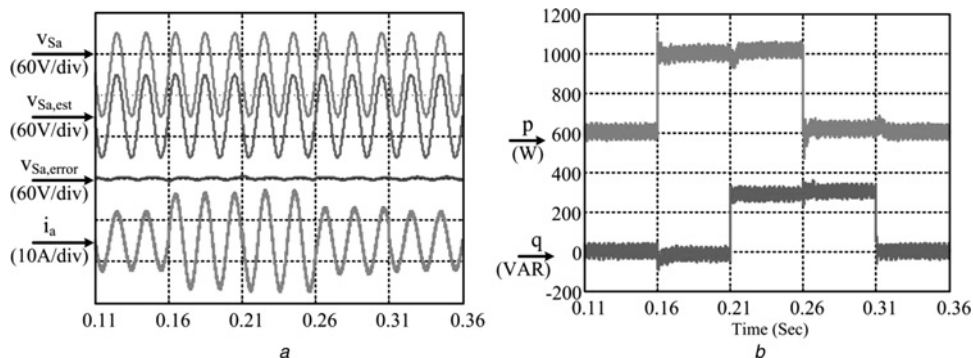


Fig. 7 Simulated transient performance of the proposed method under various step changes in the references powers

- a Grid voltage and current
- b Exchanged powers

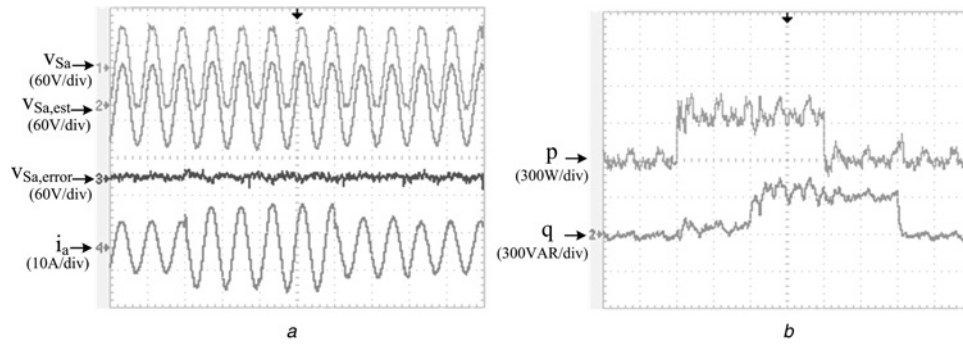


Fig. 8 Experimental transient performance of the proposed method under various step changes in the references powers
 a Grid voltage and current
 b Exchanged powers

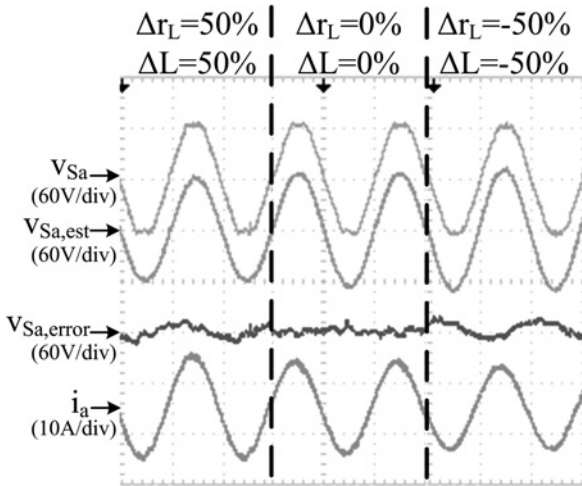


Fig. 9 Experimental results showing the robustness of the proposed method to mismatch in the filter impedance

4.1 Steady-state performance

Simulation and experimental results of the proposed control system under steady-state operation are presented in Figs. 5 and 6, respectively. As shown in Fig. 5, the proposed technique can successfully regulate the power exchange with the grid while achieving the unity power factor operation and simultaneously sinusoidal grid currents. Fig. 6 demonstrates the experimental waveforms when the grid voltage is contaminated by harmonics, listed in Fig. 6d. Apparently, the waveforms confirm the excellent performance of the proposed voltage sensorless synchronisation method, even when the grid is polluted and distorted. Fig. 6a

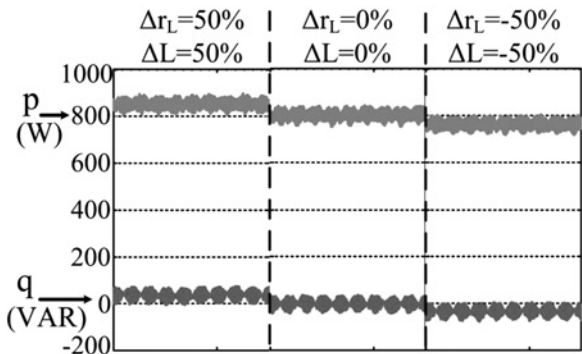


Fig. 10 Simulation results showing the robustness of the proposed method to mismatch in the filter impedance

shows that thanks to the inherent feature of resonators in the PR controller and the HC network, the proposed voltage estimator can successfully estimate fundamental component of the grid voltage. As it can be seen in Fig. 6c, the THD of the injected current is found to be 1.7%, which meets the IEEE Std 519 recommendations.

4.2 Transient performance

Simulated and experimental transient response of the proposed method under various step changes in power references is shown in Figs. 7 and 8. The results confirm the fast and decoupled

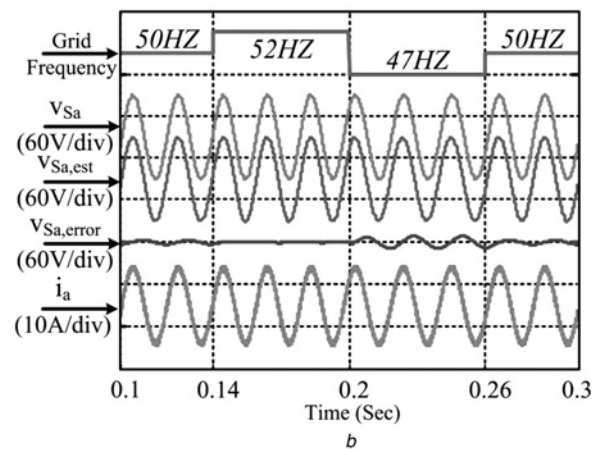
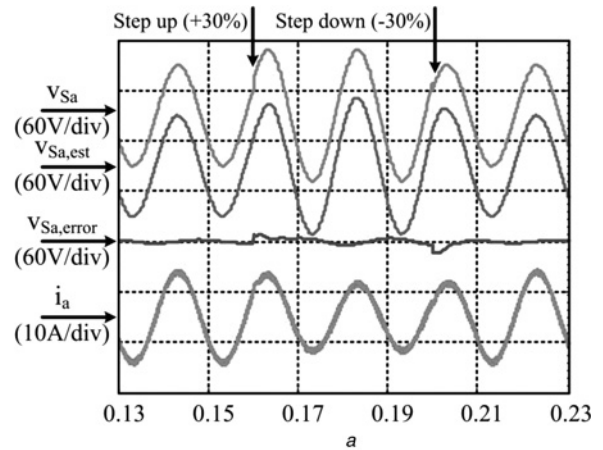


Fig. 11 Simulated performance of the proposed method under grid disturbances
 a Grid amplitude changes
 b Grid frequency changes

Table 1 Comparison among the various voltage estimation methods

Method	Algorithm complexity and computational burden	Dynamic performance	Sensitivity to measurement noises	Sensitivity to parameter mismatches	Practical difficulties
voltage estimation based on instantaneous powers [5, 6]	low	limited dynamic because of filtering action	very high	medium	1. amplification of high frequency noises because of differentiation operation 2. inability under light load conditions (near zero currents)
virtual flux [7–10]	low	limited dynamic because of integral action	low	medium	1. necessity of integral desaturation techniques
Luenberger observer [12]	high	good	low	low	1. difficulty of tuning the observer gains 2. sensitivity or even the possibility of instability in the case of improper tuning of the observer gains
Kalman filter [11]	very high	good	very low	low	1. difficulty of determining the covariance matrices 2. possibility of instability in the case of improper tuning of the filter parameters
proposed method	very low	good	medium	medium	none

control of active and reactive powers. Also, Figs. 7a and 8a prove that the voltage estimator offers an excellent transient performance, as it can successfully rebuild the estimated voltages almost instantaneously following various step transients of the reference powers.

4.3 Robustness to filter impedance uncertainties

Figs. 9 and 10 show the performance of the proposed estimation method with considering the mismatch in the filter impedance. Clearly, for a wide range of parameter mismatches the grid voltage estimator can successfully generate the grid voltage fundamental component with minimum errors. This error appears as a small deviation in the injected currents and exchanged powers from their reference values. However, the system stability is not affected at all and a stable operation under all parameter mismatch conditions is achieved.

4.4 Performance under grid disturbances

Fig. 11a shows the performance of the proposed estimation scheme in response to step changes in the grid voltage amplitude, such that the grid voltage amplitude jumps by 30% and then falls back by 30%. Also, Fig. 11b presents the converter waveforms in response to several step changes in the grid frequency. In all circumstances, the proper operation of the proposed scheme in successfully estimating the grid voltage with minimum error is obvious. Moreover, the system stability is not affected at all and stable operation under both frequency and amplitude changes is achieved.

5 Conclusion

In recent years, the possibility of replacing grid voltage sensors with a software algorithm has attracted considerable attentions because of the many advantages it offers. In this paper, a simple and efficient voltage estimation method is presented, which can be easily applied to any VSC-based power conditioning system. The proposed estimation method includes only a few simple operations, such as sums and products, and does not require any integral, derivative or trigonometric operations in its structure. A brief comparison of the proposed voltage estimation method with other state of the art techniques is presented in Table 1.

Moreover, when the PR controller is combined with the proposed voltage estimation, the grid voltage synchronisation is done without

using any PLL or BPF, even when the grid voltage is distorted and polluted. This attractive feature is achieved because of the inherent harmonic filtering of the proposed voltage estimator and the PR controller. Finally, the feasibility of the proposed method for distributed power generation systems is investigated and analytical achievements are confirmed with extensive simulations and experiments under different operating conditions.

6 References

- Teodorescu, R., Liserre, M., Rodriguez, P.: 'Grid converters for photovoltaic and wind power systems' (John Wiley & Sons, 2011)
- Zhou, Y., Huang, W., Zhao, P., Zhao, L.: 'Coupled-inductor single-stage boost inverter for grid-connected photovoltaic system', *IET Power Electron.*, 2014, 7, (2), pp. 259–270
- Gomez Jorge, S., Solsona, J., Busada, C.: 'Reduced order generalised integrator-based current controller applied to shunt active power filters', *IET Power Electron.*, 2014, 7, (5), pp. 1083–1091
- Rajendran, S., Govindarajan, U., Reuben, A., Srinivasan, A.: 'Shunt reactive VAR compensator for grid-connected induction generator in wind energy conversion systems', *IET Power Electron.*, 2013, 6, (9), pp. 1872–1883
- Noguchi, T., Tomiki, H., Kondo, S., Takahashi, I.: 'Direct power control of PWM converter without power-source voltage sensors', *IEEE Trans. Ind. Appl.*, 1998, 34, (3), pp. 473–479
- Hansen, S., Malinowski, M., Blaabjerg, F., Kazmierkowski, M.P.: 'Sensorless control strategies for PWM rectifier', Proc. Applied Power Electronics. (APEC), New Orleans, 2000, vol. 2, pp. 832–838
- Antoniewicz, P., Kazmierkowski, M.P.: 'Virtual flux based predictive direct power control of ac/dc converters with on-line inductance estimation', *IEEE Trans. Ind. Electron.*, 2008, 55, (12), pp. 4381–4390
- Kulka, A.: 'Sensorless digital control of grid connected three phase converters for renewable sources', Ph.D. dissertation, Norwegian Univ. Sci. Technol., Trondheim, Norway, 2009
- Duarte, J.L., Van Zwam, A., Wijnands, C., Vandenput, A.: 'Reference frames fit for controlling PWM rectifiers', *IEEE Trans. Ind. Electron.*, 1999, 46, (3), pp. 628–630
- Suul, J.A., Luna, A., Rodríguez, P., Undeland, T.: 'Voltage-sensor-less synchronization to unbalanced grids by frequency-adaptive virtual flux estimation', *IEEE Trans. Ind. Electron.*, 2012, 59, (7), pp. 2910–2923
- Hoffmann, N., Wilhelm, F.: 'Minimal invasive equivalent grid impedance estimation in inductive-resistive power networks using extended Kalman filter', *IEEE Trans. Power Electron.*, 2014, 29, (2), pp. 631–641
- Leon, A.E., Solsona, J.A., Valla, M.L.: 'Control strategy for hardware simplification of voltage source converter-based power applications', *IET Power Electron.*, 2011, 4, (1), pp. 39–50
- Ahmed, K.H., Massoud, A.M., Finney, S.J., Williams, B.W.: 'Sensorless current control of three-phase inverter-based distributed generation', *IEEE Trans. Power. Deliv.*, 2009, 24, (2), pp. 919–929
- Mohamed, Y.A.I., Rahman, M.A., Seethapathy, R.: 'Robust line-voltage sensorless control and synchronization of LCL-filtered distributed generation inverters for high power quality grid connection', *IEEE Trans. Power Electron.*, 2012, 27, (1), pp. 87–98
- Mohamed, Y.A.I., El-Saadany, E.F.: 'An improved deadbeat current control scheme with a novel adaptive self-tuning load model for a three phase

- PWM voltage-source inverter', *IEEE Trans. Ind. Electron.*, 2007, **54**, (2), pp. 747–759
- 16 Dai, M., Marwali, M.N., Jung, J.W., Keyhani, A.: 'Power flow control of a single distributed generation unit', *IEEE Trans. Power Electron.*, 2008, **23**, (1), pp. 322–331
- 17 Mohamed, Y.A.I., El-Saadany, E.F.: 'Adaptive discrete-time grid-voltage sensorless interfacing scheme for grid-connected DG-inverters based on neural network identification and deadbeat current regulation', *IEEE Trans. Power Electron.*, 2008, **23**, (1), pp. 308–321
- 18 Mohamed, Y.A.I., El-Saadany, E.F.: 'A robust natural-frame-based interfacing scheme for grid-connected distributed generation inverters', *IEEE Trans. Energy Convers.*, 2011, **26**, (3), pp. 728–736
- 19 Gholami-Khesht, H., Monfared, M.: 'Instantaneous grid voltage estimation based on the Newton-Raphson optimization for grid connected VSC applications', The 5th Annual Int. Power Electronics, Drive Systems and Technologies Conf. (PEDSTC 2014), 2014, pp. 66–71
- 20 Wei, Z., Chen, J., Chen, X., Gong, C., Fan, Y.: 'Modified one-cycle-controlled three-phase pulse-width modulation rectifiers under low-output', *IET Power Electron.*, 2014, **7**, (3), pp. 753–763
- 21 Qiao, C., Smedley, K.M.: 'Unified constant-frequency integration control of three-phase standard bridge boost rectifiers with power-factor correction', *IEEE Trans. Ind. Electron.*, 2003, **50**, (1), pp. 100–107
- 22 Ghodke, A., Chatterjee, K.: 'One-cycle-controlled bidirectional three-phase unity power factor ac–dc converter without having voltage sensors', *IET Power Electron.*, 2012, **5**, (9), pp. 1944–1955
- 23 Yazdani, A., Iravani, R.: 'Voltage-sourced converters in power systems' (Wiley, 2010)
- 24 Li, B., Yao, W., Hang, L., Tolbert, L.M.: 'Robust proportional resonant regulator for grid-connected voltage source inverter (VSI) using direct pole placement design method', *IET Power Electron.*, 2012, **5**, (8), pp. 1367
- 25 Timbus, A., Liserre, M., Teodorescu, R., Rodriguez, P., Blaabjerg, F.: 'Evaluation of current controllers for distributed power generation systems', *IEEE Trans. Power Electron.*, 2009, **24**, (3), pp. 654–664
- 26 Zmood, D.N., Holmes, D.G.: 'Stationary frame current regulation of PWM inverters with zero steady-state error', *IEEE Trans. Power Electron.*, 2003, **18**, (3), pp. 814–822
- 27 Blaabjerg, F., Teodorescu, R., Liserre, M., Timbus, A.: 'Overview of control and grid synchronization for distributed power generation systems', *IEEE Trans. Ind. Electron.*, 2006, **53**, (5), pp. 1398–1409
- 28 Castilla, M., Miret, J., Matas, J., Garcia de Vicuña, L., Guerrero, J.M.: 'Linear current control scheme with series resonant harmonic compensator for single-phase grid-connected photovoltaic inverters', *IEEE Trans. Ind. Electron.*, 2008, **55**, (7), pp. 2724–2733
- 29 Castilla, M., Miret, J., Matas, J., Garcia de Vicuña, L., Guerrero, J.M.: 'Control design guidelines for single-phase grid-connected photovoltaic inverters with damped resonant harmonic compensators', *IEEE Trans. Ind. Electron.*, 2009, **56**, (11), pp. 4492–4501
- 30 Vidal, A., Freijedo, F., Yepes, A., *et al.*: 'Assessment and optimization of the transient response of proportional-resonant current controllers for distributed power generation systems', *IEEE Trans. Power Electron.*, 2013, **60**, (4), pp. 1367–1383
- 31 Monfared, M., Golestan, S., Guerrero, J.M.: 'Analysis, design, and experimental verification of a synchronous reference frame voltage control for single-phase inverters', *IEEE Trans. Ind. Electron.*, 2014, **61**, (1), pp. 258–269
- 32 Yepes, A., Freijedo, F., Doval-Gandoy, J., Lopez, O., Malvar, J., Fernandez-Comesana, P.: 'Effects of discretization methods on the performance of resonant controllers', *IEEE Trans. Power Electron.*, 2010, **25**, (7), pp. 1692–1712
- 33 Yuan, X., Merk, W., Stemmler, H., Allmeling, J.: 'Stationary-frame generalized integrators for current control of active power filters with zero steady-state error for current harmonics of concern under unbalanced and distorted operating conditions', *IEEE Trans. Ind. Appl.*, 2002, **38**, (2), pp. 523–532